INVESTIGATION OF NOVEL METALLIZED MONOPROPELLANTS

M. Kurilov [(1)] [(*)], C.U. Kirchberger [(1)], D. Freudenmann [(1)], S. Ricker [(1)], H. K. Ciezki [(1)], S. Schlechtriem [(1)]
[(1)] German Aerospace Center (DLR), Institute of Space Propulsion,
Langer Grund, 74239 Hardthausen, Germany
[(*)] Corresponding author, email: maxim.kurilov@dlr.de

KEYWORDS: energetic materials, booster propulsion, rocket propulsion, gelled propellants, homogenous slurry propellants, slurry, metal combustion, solid propellant, monopropellant, green propulsion, new propellants

ABSTRACT:

High energy high density metallized monopropellants called homogeneous slurry propellants (HSP) are being developed at DLR. In theory, this propellant class has significant advantages, however because HSPs contain many components a detailed characterization of the combustion behavior is necessary. In this study, we evaluate how the base fluid affects combustion performance from model rocket combustion chamber experiments. Additionally, combustion residues were analyzed with thermogravimetric methods. It was found that the use of an energetic base liquid not only enhances the energy content but also is obligatory to achieve a high combustion efficiency and to minimize the amount of combustion residues in the chamber. Furthermore, hints to the underlying combustion mechanisms were identified. Especially, the role of the propellant evaporation process, which is the prerequisite for fully-fledged combustion in HSPs, was determined.

1. INTRODUCTION

Gelled monopropellants, oxidizers and fuels potentially offer significant benefits compared to conventional solid, liquid or hybrid propellants. Therefore, in Germany a development program on that topic was started in the early 2000s. The motivation for this is the unique features gelled propellants possess. These make them perfect candidates for certain application niches. In [1] a detailed description of the German gel program along with typical application descriptions can be found. In [2] further aspects of gel propellant research especially in the field of rheology, spray/injection and combustion at DLR Institute of Space Propulsion are depicted. Both references also analyze in detail which advantages gelled propellants have to offer. In the following paragraph we will discuss the two most important ones.

The strongest assets gelation of energetic materials entails is the altering of the rheological behavior: these thickened liquids with a distinct yield point behave like solids at rest [3]. This improves handling and storage properties since the propellant neither can be accidently spilled nor it can leak out and form pools that potentially can be the source of fires [4]. Additionally, altering rheological properties allow for incorporation of metal fuels ([5], [6]), energetic materials ([7], [8]) and combustion and ignition catalysts ([9], [10]). By this means energy density and combustion properties of gelled propellants can be enhanced and/or tailored. This however comes at a price: the flow properties become non-Newtonian. This is because of (sometimes even time dependent) interactions within the gel microstructure when a force is applied, i.e. during a flow process. This can lead to unfavorable flow regimes ([3], [11]). However, if base liquid and gellator are matched in a specific way, pressure losses during flow may even be lower than in Newtonian liquids [11]. Additionally, injection and spray behavior especially in impinging jet injectors may become negatively affected. This can require higher backpressures than in liquid propellants to ensure proper atomization ([11], [12]) or in spray regimes that can produce elongated threads instead of droplets ([13], [14]). Nevertheless, as showed in [12], [15] and [16] sufficient atomization may also be reached.

An important driver of the German research activities in this field is the endeavor for environmentally friendly low health hazard gelled propellants. This not only leads to a lower handling hazard potential and thus helps to lower overall product and procedure costs. Reference [4] shows this in more detail for the “GRP” gelled monopropellant family. In [10] a screening method originally developed for but not limited to environmentally friendly low health hazard gelled hypergolic oxidizers and fuels is presented.

2. HOMOGENOUS SLURRY PROPELLANTS

More recently, research focus at DLR was shifted towards versatile metallized high-impulse high-density propellants for booster, sustainer and kick-stage applications. The aim of these activities is to create propellants which allow to combine the flexibility of liquid rocket engines with volumetric energy density of solid rocket motors. These propellants belong to a group of substances somewhat different than typical propellant gels. Requirements concerning rheological properties in this class of substances are relaxed compared to classical gels. The so-called homogenous slurry

Table 1: Propellant composition

Name	Base fluid	Metal fuel	Gellator	Additives
HSP201	Non-energetic	<20%	Organic	Oxidizer
HSP312	Energetic	<20%	Organic and non-organic	Oxidizer, desensi-tizer

propellants (HSPs) – a term coined by our research group – do not necessarily possess a district yield point. This means incorporated particles such as metal fuels will eventually settle. This however may take a long time since the viscosity of the propellant is increased at rest because of its non-Newtonian rheological properties. The duration of that time span usually depends on the production process and on the amount of added gellator. By tailoring the propellant composition to mission requirements, the negative impact on flow, spray and combustion performance usually attributed to gelled propellants may be minimized. For example, in a tactical missile long term propellant stability is required. To achieve this, a high gellator amount must be added. In a commercial launcher system which is intended to be launched within several weeks significantly less gellator is sufficient. Another approach to further boost volumetric and gravimetric impulse performance our group pursues is the addition of oxidizers. This is done to improve the overall oxygen balance in the propellant formulation and to further enhance the energy content.

To explore combustion properties of two HSPs, a test campaign at the M11 test bench was carried out. The aim of this campaign was to rapidly assess the impact of various propellant components on combustion performance. In this paper we will present some outcomes regarding the impact of the base fluids on combustion performance. In this context an energetic base fluid has similar properties than a monopropellant. A non-energetic base fluid is regarded as an inert substance such as a hydrocarbon or water. In Table 1 two HSPs with similar composition but different base fluids are presented.

3. TEST SETUP AND DATA EVALUATION

The experimental campaign was carried out at test bench M11.4 of the M11 test complex. This test bench is specially dedicated to experiments with gelled propellants. The propellant is fed into the injector by means of a piston which is actuated by a hydraulic actuator capable of delivering up to 180 kN of force. The propellant mass flow is

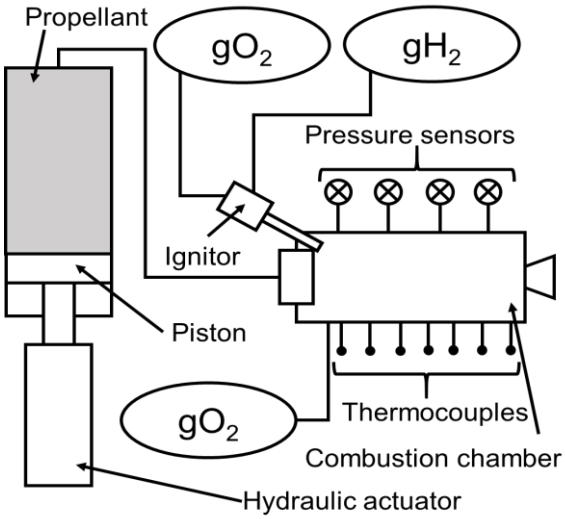

Figure 1: Combustion test setup

calculated from the piston drive speed and propellant density. As a means of ignition, a two-stage hydrogen/oxygen gas torch is used. During the first stage operation a fuel-rich hot hydrogen/oxygen plasma is produced in a pre-combustor. This mixture is injected into the main combustion chamber near the injector face. Then, as the second stage, oxygen is directly injected into the (main) combustion chamber. This stage is also referred to as the boost oxygen stage.

Even though the overall ignitor mass flow never exceeds several grams per second, this approach proved as a reliable source of ignition. Because the overall ignition gas mass flow is small compared to the main chamber mass flow (10 – 100 times the gas torch mass flow) and typically is cut off after a short time it is neglected in mass flow calculations. At M11.4 all gasses may be delivered at a pressure of up to 200 bar, however usually lower pressure levels are used. In all tests described here all gasses were delivered at 45 to 48 bar. Due to material tear and wear three similar combustion chambers (see Tab. 2) were used throughout the campaign. Also because of irreparable damage we had to change the injector during the campaign. Both injectors had the same total flow-through area. In every test we used the same nozzle segment, i.e. the nozzle throat choke area was kept the same in all tests. The most important parameters of the combustion experiments carried out are summarized in Table 2: Experimental setup parameters. An overview of the combustion test setup is provided in Fig. 1.

All chambers are equipped with K-type thermocouples and Kistler 4043A20 100 bar pressure transducers. The thermocouples are located in bores ending 1 mm above the combustion chamber inner wall. To achieve a stable and reproducible material contact the thermocouples are held in place by springs in a

Table 2: Experimental setup parameters

#	Imping jet injector type	Combustion chamber	Material	ID [mm]	OD [mm]	L [mm]	Thermo-couples	Pressure sensors	Propellant
1	Triplet	BK40ZS	Stainless steel	40	56	195	8	4	HSP201
2	Doublet	BK40	Stainless steel	40	56	195	8	5	HSP201
3	Doublet	BK40	Stainless steel	40	56	195	8	4	HSP312
4	Doublet	BK40ATM	Inconel	40	58	195	n. a.	1	HSP312

Table 3: TGA data of combustion residues

	Overall mass change below 120°C		Overall mass change 120 - 500°C		Overall mass change 500 – 1000°C	
Measurement no. →	1	2	1	2	1	2
Test 1	-3.13%	-2.2%	-11.53%	-9.78%	-0.09%	1.43%
Test 2	-8.24%	-6.51%	-7.84%	-9.12%	3.47%	1.54%
Test 3	-1.81%	-1.30%	-0.49%	-0.38%	-0.94%	-0.70%
Test 4	0.94%	-0.18%	-0.50%	-0.57%	-0.39%	-0.45%

similar manner as described in [17].

Pressure signals from the sensors are amplified in DEWETRON amplifiers and are then conducted to a NI-PXI data acquisition system. Pressure signal data rate is 20 kHz. The thermocouples are cold junction compensated using a Klasmeier “ice box” but otherwise directly wired to NI-PXI low frequency data acquisition modules. Data rate for temperature signals is 4 kHz.

Thermogravimetric analysis (TGA) and deferential scanning calorimetry (DSC) of the residues from the combustion experiments were performed by a NETSCH STA 449F3 apparatus. The samples were heated with 10 K/min in Al_2O_3 crucibles. The measurements were carried out inside an oxygen atmosphere. The measurements were repeated once.

4. COMBUSTION ANALYSIS METHODOLOGY

We evaluate combustion performance by means of comparing the theoretically calculated characteristic velocity C^*_{theo} with the measured C^*_{exp} value. The theoretical value is calculated by evaluating an equilibrium flow rocket problem at measured combustion pressure in Gordon-McBride NASA CEA computer program [18]. The experimental value is calculated from the minimal throat area A_t, the measured stagnation pressure p_c and the propellant mass flow $\dot{m}$ (equation Eq. 1). Combustion efficiency is then determined by Eq. 2.

$$C^*_{exp} = \frac{\dot{m} * p_c}{A_t} \qquad \text{Eq. 1}$$

$$\eta_{C^*} = \frac{C^*_{exp}}{C^*_{theo}} * 100\% \qquad \text{Eq. 2}$$

Experimental characteristic velocity was calculated from an average mass flow and an average determined within an evaluation window of 1000 ms. In each case the averaging window is placed shortly after the end of the first ignitor operating stage (at about 3500 – 4500 ms). At this point of time the nozzle is considered unobstructed by combustion product residues and thus no correction for this effect needs to be applied.

The axial heat flow distribution is calculated from thermocouple readings. To get “quasi-steady state” values the same methodology is used as described in [19]. In all tests the temperature gradient dT/dt for each thermocouple was calculated and then averaged between 4800 and 5800 ms. We consider the temperature gradient spatial distribution to be fully developed at this point of time, i.e. heating of the chamber material is proceeding in a uniform manner. This makes it possible to apply the Fourier Law for calculate the wall heat flow (Eq. 3).

The only additional information required are the

geometrical dimensions, i.e. inner (r_i) and outer (r_o) combustion chamber radii, the density $\rho_{wall}(T)$ and the specific heat capacity $c_{wall}(T)$ of the chamber material. Temperature dependent material data for stainless steel was calculated with the help of data provided by [20]. Even though this is a very simple approach it has been verified against more sophisticated analysis methods in [19] to correctly represent the qualitative axial heat flux distribution in a rocket combustion chamber and to also get a fair estimation of the actual quantitative values.

$$\dot{q}_{in} = \rho_{wall}(T) * c_{wall}(T) * \frac{{r_o}^2 - {r_i}^2}{2 * r_o} * \frac{dT}{dt} \qquad \text{Eq. 3}$$

There are however limitations to our evaluation approach. Combustion of metal fuels an energetic substances is known to be strongly affected by chamber pressure. This however is not implemented in detail in CEA. Therefore, the characteristic velocity may be predicted incorrectly by CEA. This can lead to overestimation of the combustion performance, i.e. combustion efficiency values even greater than 100% can be achieved. Additionally, during combustion not only gaseous but also liquid and solid products are produced. This may change the nozzle throat area, i.e. the nozzle may partly become obstructed during a test run. In this case combustion efficiency measurements may be imprecise. The heat flow calculation may also be not ideal since transversal heat conduction is neglected and the temperature gradient distribution may still be subject to changes after or during the evaluation window. Nevertheless, we are confident that combining the proposed methods will help us to deduce and assess the physical processes occurring during combustion.

5. RESULTS AND DISCUSSION

5.1. Test 1

Pressure readings of test 1 are depicted in Fig. 2. During the first test the second ignitor stage (POIGN in diagram) was kept running after the first ignition stage finished operating (POZ in diagram). That is to say for the whole test duration several grams per second of oxygen were injected into the combustor near the injector face. This was done to make sure that the first test with HSP201 runs smoothly and combustion is not quenched and no dangerous propellant accumulations or hard restarts of the combustion chamber may occur. The ignition procedure resulted in a (lower than expected) stable pressure level of 25 – 30 bar.

The combustion chamber pressure is designated as PBKAVG in Fig. 2. Combustion efficiency between 3500 and 4500 ms was calculated to be 55%. Later pressure steadily rose to 40 bar. This is attributed to combustion residues and unburnt propellant accumulating within the nozzle section and partly reducing the throat diameter (see Fig. 6 and 7).

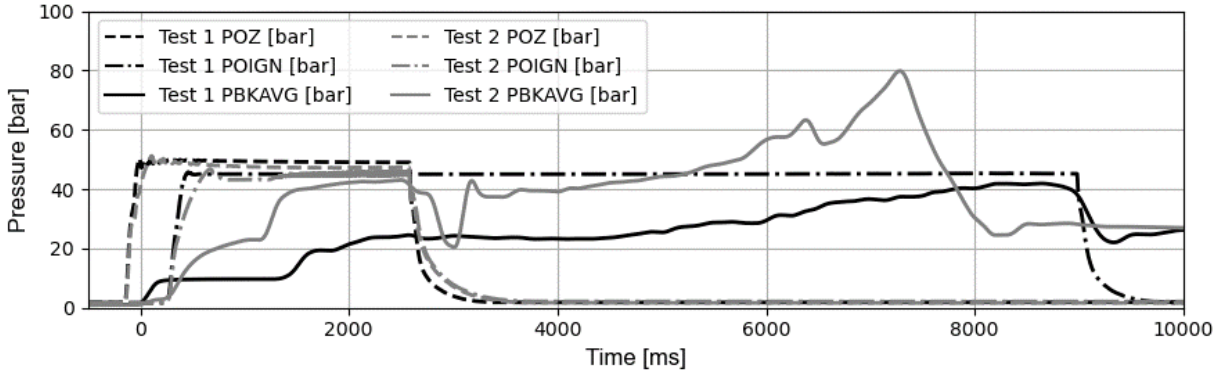

Figure 2: Pressure readings in test 1 & 2

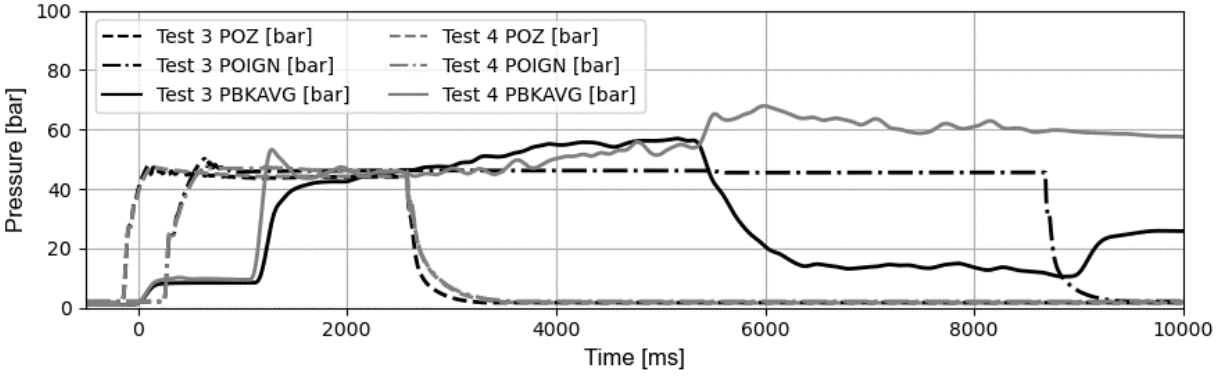

Figure 3: Pressure readings in test 3 & 4

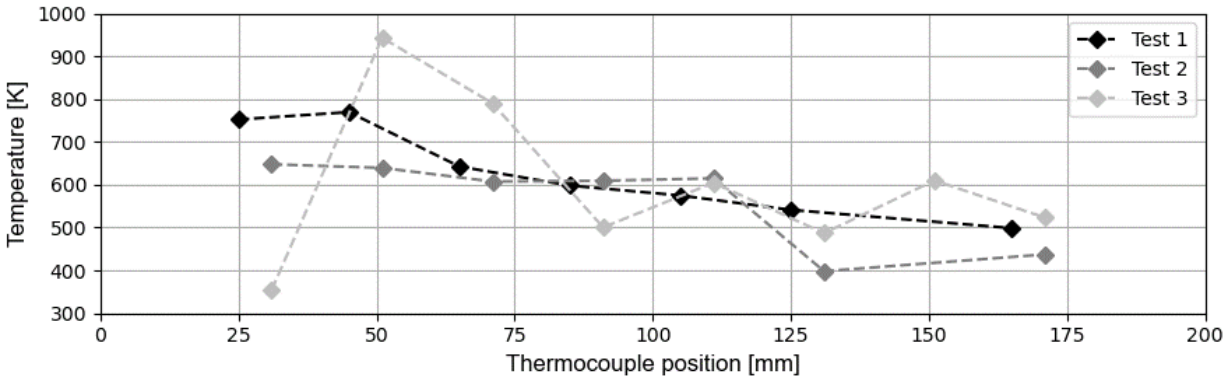

Figure 4: Axial wall temperature in tests 1, 2 & 3

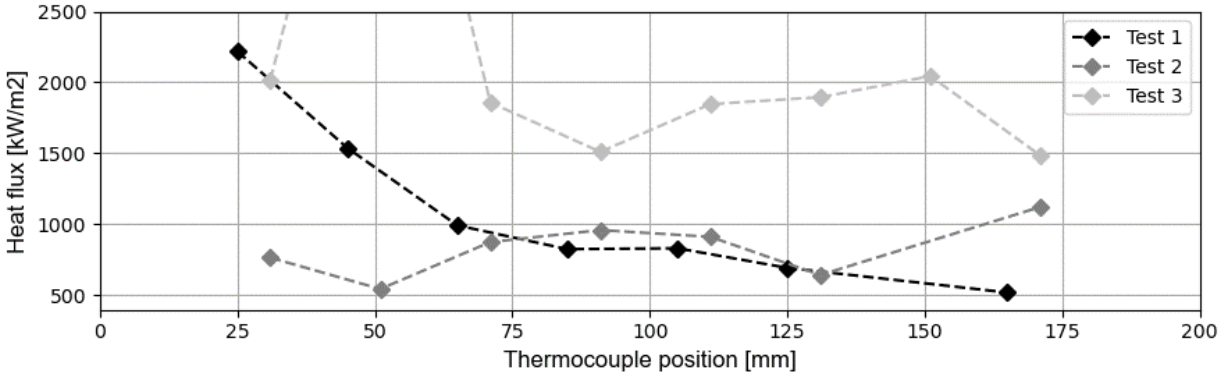

Figure 5: Axial heat flux distribution in tests 1, 2 & 3

Within the first 50 mm from the injector face the measured structure temperature is around 800 K. Then a continuous drop to around 500 K towards the nozzle section occurs (see Fig. 4). The heat flux also has its maximal value of about 2.4 MW/m2 right next to the injector face (see Fig. 5). Then a slowly declining level of around 1 MW/m2 is reached. Both, the temperature and the heat flow distribution clearly indicate that a hot-spot is located near the injector face. The position of this hot-spot correlates with the position of the ignition boost oxygen feeding ports. Unfortunately, the triplet injector was damaged in this test and thus was no longer available during the test campaign. Additionally, due to a design issue with the oxygen inlet ports the combustion chamber also was damaged.

The TGA of the combustion residues (see Tab. 3) shows a high mass loss between 120 and 500°C. This indicates organic substances and residual oxidizer decomposition. The mass loss below 120°C is mainly attributed to water evaporation. Above 500°C there is a slight mass gain in the second measurement which is interpreted as metal fuel residues reacting to metal oxides in the oxygen atmosphere. Both the mass loss between 120 and 500°C and the mass gain above 500°C supports the hypothesis that combustion was poor in this test. This is also supported by the low estimated efficiency and, decreasing temperatures and heat flows towards the nozzle segment.

5.2. Test 2

Because the combustion chamber used in test 1 was damaged, a different but very similar chamber was used instead. Additionally, in the second test run with HSP201 a doublet impinging jet injector with the same injection area as the triplet injector from test 1 was used. This type of injector is known to have a similar atomization performance as the triplet injector used in test 1. In this test propellant mass flow was roughly 20% higher than in test 1. We think these two factors along with some unburnt propellant from a misfire before lead to a much higher initial pressure rise in this test than in test 1. Here a pressure level of more than 40 bar is reached during the ignitor operating phase (1000 ms – 2500 ms).

This time the ignition boost stage was switched off at the 2500 ms mark. After that, the combustion pressure sharply drops to 20 bar but then recovers again (see Fig. 2). We interpret this as the combustion process almost losing its self-sustainability. Combustion efficiency was estimated from the time interval after this event but before the onset of the steady pressure rise to 80 bar which eventually triggered an over-pressurization redline. Between 3500 and 4500 ms average combustion efficiency was 76%. In case of test 2 it is however not safe to say the nozzle was entirely unobstructed between 3500 and 4500 ms. This is because combustion was nearly extinguished shortly before and unburnt propellant was probably sitting in the

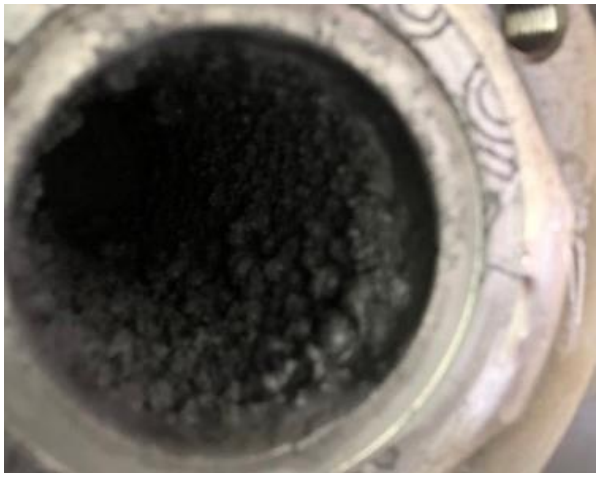

Figure 6: Residues in combustion chamber after test 1

Figure 7: Residues in nozzle segment after test 1

Figure 8: Residues in combustion chamber after test 2

Figure 9: Residues in nozzle segment after test 2

nozzle section partially blocking the throat area. Therefore, actual combustion efficiency may have been lower.

Despite a higher mass flow the measured wall temperatures are lower in this test. The values are declining along the combustor axis from 670 K near the injector face to approx. 450 K near the nozzle section. The heat flux distribution is entirely different than in test 1. Here the values steadily rise from 800 – 600 kW/m^2 near the injector face to just above 1 MW/m^2 halfway through the combustor (which is somewhat higher than in test 1 at the same position) and then falls again towards the nozzle section to a 700 kW/m^2 level. We interpret this as the main combustion zone being located further downstream and being less distinct than in test 1. After the test a higher amount of residue was found in the combustion chamber than in test 1 (see Fig. 8 and 9). This also supports the assumption that combustion in test 2 was not as intensive as in test 1.

The quite high mass loss (see Tab. 2) between 120 and 500°C and the high mass gain above 500°C indicates a low degree of propellant oxidation. Especially above 500°C where metal oxidation takes place the mass gain is higher than for test 1. From this result it may be deduced that in test 2 less metal was oxidized than in test 1. This substantiates the hypothesis that in test 2 combustion performance was poorer than in test 1.

5.3. Test 3

Test 3 was carried out with the same combustion chamber and injector as in test 2. However, a different propellant was used – the most significant change was the use of a different base fluid. This time an energetic base fluid was used instead of a non-energetic one. The other ingredients were kept in similar proportions (see Tab. 1). Again, as in test 1, the ignition boost oxygen was left running to avoid extinguishing and/or hard restarts.

At the beginning of the ignition phase pressure smoothly rose to 42 bar but then slowly continued to rise to about 56 bar. This pressure rise is mainly attributed to accumulation of combustion residues in the nozzle segment, which led to a gradual reduction of the throat diameter (see Fig. 3). Then at approx. 5300 ms a burn through of the combustion chamber wall near the injector face occurred. This caused the pressure to drop but without extinguishing combustion. Again,

Figure 10 Residues in combustion chamber after test 3

Figure 11: Residues in nozzle segment after test 3

Figure 12: Residues in combustion chamber after test 4

combustion efficiency was calculated from the interval between 3500 and 4500 ms and resulted in 106%. A such high value may be attributed to combustion mechanisms not implemented in CEA but here we assume the gradual obstruction of the nozzle throat had an even higher impact.

Temperatures and mass flows in test 3 are higher than in test 1 & 2. After reaching 1000 K near the injector face the temperature drops and stays in the 520 – 620 K range in the second half of the combustor (see Fig. 4). Heat flux also spikes near the injector face to over 4 MW/m^2 then drops to the 1.3 MW/m^2 area to form a second maximum at about 2 MW/m^2 (see Fig. 5). This may indicate a second combustion zone. Similarly, as in test 1 wall heat flux and temperature maxima in the first third of the combustion chamber are most certainly caused by the boost oxygen injection

After the test a thin light grey-whitish brittle layer was found on the combustion chamber walls and in the nozzle section (see Fig. 11 and 12). The nozzle throat was only slightly obstructed. It is however not clear how much of the depositions occurred during the test and how much resulted from the cooldown phase through solidification of liquid combustion products after the test.

The TGA trace shows only minor reactions except for the mass loss below 120°C which is entirely attributed to water evaporation. Because no mass gain could be detected above 500°C it is assumed all of the metal fuel has reacted. This underpins that combustion efficiency was very high.

5.4. Test 4

Since the combustion chamber was damaged again, a new one was manufactured. This chamber is ALM-manufactured from Inconel and therefore the material and geometry differ to a high degree compared to the other chambers. Readings and heat flow calculations are not presented here because these values would not be comparable to the ones in tests 1, 2 and 3.

Right after ignition pressure rapidly rises to the 50 – 55 bar level. Unlike as in test 2 there is no drop to a lower pressure level after ignition boost oxygen is switched off. Instead a comparatively steady combustion takes place. At about 5700 ms a rapid pressure rise to almost 70 bar is apparent followed a decline to 62 bar. This might be attributed to blockage of the feed line by inhomogeneities in the propellant resulting from the production process which led to a short overshoot of the injected propellant. Steady state combustion efficiency measured between 3500 and 4500 ms is 95%. Even though a slight obstruction of the nozzle throat cannot be ruled out at this point this value seems to be realistic. This assumption is further supported by a low amount of residue found in the combustion chamber after the test (see Fig. 12). Additionally, neither significant mass loss between 120 and 500°C, nor mass gain after 500°C was found by the TGA of these residues, which show that the propellant almost completely reacted during the combustion process.

5.5. Influence of the base fluid on combustion

An approach to explain the results obtained in this test campaign is to look into the role of the HSP base liquid. Since HSPs are very similar to gelled propellants we do not expect the combustion behavior to be totally different. Even though gelled propellants possess a multitude of complicated

combustion mechanisms it is generally agreed upon that solid or semisolid components in these propellants only can undergo fully-fledged combustion if the base liquid is evaporated (see [8], [21], [22]).

In test 2 the non-energetic base liquid only evaporates as a result of the heat transferred from the combustion zone further downwards. Since vapors produced by non-energetic substance do not react at low temperature a vapor rich cold zone near the injector face is formed. Therefore, the evaporation process, which is a prerequisite for fully-fledged combustion, takes a very long time. If some of these slowly evaporating droplets hit the combustion chamber wall evaporation ceases and the propellant is no longer contributing to the combustion process. Combustion is therefore incomplete and unburnt propellant can be found inside the combustor after the test. In test 1 there is a hot zone produced through gaseous oxygen injection. Even though only several grams per second are injected the evaporation process of the non-energetic base fluid is much faster than in test 2. Therefore, less residues are accumulated in the combustion chamber. Combustion is however still incomplete.

In test 4 an energetic base fluid is used. Here right after the evaporation sets on the propellant vapors around the droplets immediately start to combust. Heat produced in this reaction facilitates the evaporation process. Eventually, fully-fledged metal combustion takes place earlier since evaporation is faster. A high degree of oxidation of combustion residues and a much lower amount thereof than in tests 1 & 2 supports this hypothesis. In test 3 the evaporation process is further amplified by the boost oxygen injection. The oxygen together with the combusting energetic base fluid leads to a very high heat flux in the first third of the combustion chamber. The secondary heat flow maximum which is located in the second half of the combustion chamber may be attributed to a metal combustion zone. This however needs to be verified in further experiments. In test 4 the combustion also was self-sustaining and not much residues were produced even though no boost oxygen was injected after the end of ignitor operation phase.

6. CONCLUSION

A new class of high impulse metallized propellants called HSPs is being developed at the DLR Institute for Space Propulsion. The aim of the program is to create a new class of monopropellants which combine the flexibility of liquid propellants with the impulse density and good handling properties of solid propellants. The focus of the hot fire campaign was to assess the influence of the base fluid on the HSP combustion behavior. Two similar HSPs each containing a metal fuel and an oxidizer were fired in a model rocket combustion chamber. One HSP had a non-energetic base fluid whereas the other one had an energetic one. Additionally, TGA measurements of the residues left over from combustion were carried out.

The conducted tests showed that an energetic base fluid is beneficial since a better combustion efficiency with an acceptable amount of combustion residues can be achieved. In tests with the HSP based on a non-energetic compound only insufficient combustion performance was gained. Additionally, an unacceptably high amount of combustion residues and unburnt propellant accumulated in the combustion chamber. In one case this eventually led to total nozzle throat blockage. Moreover, TGA of the combustion residues not only shows that high temperature reactions of metal fuel leftovers can be found in the case of a non-energetic fluid but also unreacted organics and oxidizer residues.

By carefully comparing non-energetic base fluid tests with and without oxygen boost the role of base fluid evaporation and combustion could be deduced: Combustion of the HSP with the non-energetic base fluid produced less residues if the ignition boost oxygen was left running rather than if it was switched off. Additionally, TGA measurements hint to a higher degree of metal oxidation with boost oxygen left running. From this outcome and from temperature and heat flow measurements it was figured that a hot spot near the oxygen injection ports beneficially influenced propellant evaporation. Consequently, more material reacted before hitting the walls and thus being rendered unavailable for further reaction. This is further undermined by the outcomes with an energetic base fluid. Here, the fluid immediately begins to combust as soon propellant evaporation begins. This accelerates the evaporation process in the beginning and leads to a better overall combustion performance. This is supported by TGA findings which indicate an almost complete metal oxidation.

In conclusion it can be outlined that in order to facilitate HSP combustion, it is crucial to accelerate the base fluid evaporation process. A very sensible possibility to achieve this is it to use an energetic base fluid. Additionally, using an energetic component instead of a non-energetic one enhances the overall energy content of the propellant mixture.

7. REFERENCES

1. Ciezki, H. K., Kirchberger, C., Stiefel, A., Kröger, P., Pinto, P. C., Ramsel, J., & Weiser, V. (2017). Overview on the german gel propulsion technology activities: Status 2017 and outlook. In *Proceedings of the 7th European Conference for Aeronautics and Space Sciences*.

2. Kirchberger, C., Kurilov, M., Stiefel, A., Freudenmann, D., & Ciezki, H. (2019). Investigations on Rheology, Spray and Combustion Processes of Gelled Propellants at DLR Lampoldshausen. In *Proceedings of the 8th European Conference for Aeronautics and Space Sciences*.

3. Madlener, K., & Ciezki, H. K. (2012). Estimation of flow properties of gelled fuels with regard to propulsion systems. *Journal of Propulsion and Power*, *28*(1), 113-121.

4. Ciezki, H. K., & Naumann, K. W. (2016). Some aspects on safety and environmental impact of the German green gel propulsion technology. *Propellants, Explosives, Pyrotechnics*, *41*(3), 539-547.

5. Negri, M., & Ciezki, H. K. (2015). Combustion of gelled propellants containing microsized and nanosized aluminium particles. *Journal of Propulsion and Power*, *31*(1), 400-407.

6. Glushkov, D. O., Kuznetsov, G. V., Nigay, A. G., & Yashutina, O. S. (2019). Heat and mass transfer induced by the ignition of single gel propellant droplets. *Journal of the Energy Institute*, *92*(6), 1944-1955.

7. Solomon, Y., Grinstein, D., & Natan, B. (2016). Active boron dispersion and ignition in gel droplet. *International Journal of Energetic Materials and Chemical Propulsion*, *15*(3).

8. Solomon, Y., Grinstein, D., & Natan, B. (2018). Dispersion of boron particles from a burning gel droplet. *Journal of Propulsion and Power*, *34*(6), 1586-1595.

9. Ricker, S., Kurilov, M., Freudenmann, D., Kirchberger, C., Hertel, T., Ciezki, H., & Schlechtriem, S. (2019). Novel gelled fuels containing nanoparticles as hypergolic bipropellants with HTP. In *Proceedings of the 8th European Conference for Aeronautics and Space Sciences*.

10. Kurilov, M., Kirchberger, C. U., Freudenmann, D., Stiefel, A. D., & Ciezki, H. K. (2018). A Method for Screening and Identification of Green Hypergolic Bipropellants. *International Journal of Energetic Materials and Chemical Propulsion*, *17*(3).

11. Stiefel, A. D., Kirchberger, C. U., Ciezki, H. K., Kurilov, M., & Kurth, G. (2020). The Flow of Gels through a Nozzle-like Geometry. *International Journal of Energetic Materials and Chemical Propulsion*, *19*(1).

12. Von Kampen, J., Alberio, F., & Ciezki, H. K. (2007). Spray and combustion characteristics of aluminized gelled fuels with an impinging jet injector. *Aerospace science and technology*, *11*(1), 77-83.

13. Negri, M., Ciezki, H. K., & Schlechtriem, S. (2013). Spray behavior of non-Newtonian fluids: Correlation between rheological measurements and droplets/threads formation. *Progress in propulsion physics*, *4*, 271-290.

14. Negri, M., & Ciezki, H. K. (2015). Effect of elasticity of Boger fluids on the atomization behavior of an impinging jet injector. *Atomization and Sprays*, *25*(8).

15. Baek, G., Kim, S., Han, J., & Kim, C. (2011). Atomization characteristics of impinging jets of gel material containing nanoparticles. *Journal of Non-Newtonian Fluid Mechanics*, *166*(21-22), 1272-1285.

16. Wang, F. S., Chen, J., Zhang, T., Guan, H. S., & Li, H. M. (2020). Experimental Study on Spray Characteristics of ADN/Water Based Gel Propellant with Impinging Jet Injectors. *Propellants, Explosives, Pyrotechnics*, *45*(9), 1357-1365.

17. Suslov, D., Woschnak, A., Sender, J., Oschwald, M., & Haidn, O. (2003, July). Test specimen design and measurement technique for investigation of heat transfer processes in cooling channels of rocket engines under real thermal conditions. In *39th AIAA/ASME/SAE/ ASEE Joint Propulsion Conference and Exhibit* (Paper No. AIAA 2003-4613).

18. McBride, B. J. (1996). *Computer program for calculation of complex chemical equilibrium compositions and applications* (Vol. 2). NASA Lewis Research Center.

19. Celano, M. P., Silvestri, S., Pauw, J., Perakis, N., Schily, F., Suslov, D., & Haidn, O. J. (2015). Heat flux evaluation methods for a single element heat-sink chamber. In *6th European Conference of Aeronautics and Space Science, Krakow, Poland*.

20. Pichler, P., Simonds, B. J., Sowards, J. W., & Pottlacher, G. (2020). Measurements of thermophysical properties of solid and liquid NIST SRM 316L stainless steel. *Journal of Materials Science*, *55*(9), 4081-4093.

21. Lee, A., & Law, C. K. (1991). Gasification and shell characteristics in slurry droplet burning. *Combustion and Flame*, *85*(1-2), 77-93.

22. Solomon, Y., DeFini, S. J., Pourpoint, T. L., & Anderson, W. E. (2013). Gelled monomethyl hydrazine hypergolic droplet investigation. *Journal of Propulsion and Power*, *29*(1), 79-86.